

# Constraints upon the CKM angle $\phi_2$ from Belle and BaBar

A. J. Schwartz<sup>a</sup>

<sup>a</sup> Physics Department  
University of Cincinnati  
P.O. Box 210011  
Cincinnati, Ohio 45221

The Belle and BaBar experiments have measured branching fractions and  $CP$  asymmetries in the charmless decay modes  $B^0 \rightarrow \pi^+\pi^-$ ,  $B^0 \rightarrow \rho^\pm\pi^\mp$ , and  $B^0 \rightarrow \rho^+\rho^-$ . From these measurements, constraints upon the CKM angle  $\phi_2$  can be obtained. These constraints consistently indicate that  $\phi_2$  is around  $100^\circ$ .

## 1. INTRODUCTION

The Standard Model predicts  $CP$  violation to occur in  $B^0$  meson decays owing to a complex phase in the  $3 \times 3$  Cabibbo-Kobayashi-Maskawa (CKM) mixing matrix. This phase is illustrated by plotting the unitarity condition  $V_{ub}^*V_{ud} + V_{cb}^*V_{cd} + V_{tb}^*V_{td} = 0$  as vectors in the complex plane: the phase results in a triangle of nonzero height. One interior angle of the triangle, denoted  $\phi_1$  or  $\beta$ , is determined from  $B^0 \rightarrow J/\psi K^0$  decays.<sup>1</sup> Another interior angle,  $\phi_2$  or  $\alpha$ , is determined from charmless decays such as  $B^0 \rightarrow \pi^+\pi^-$ ,  $B^0 \rightarrow \rho^+\pi^-$ , and  $B^0 \rightarrow \rho^+\rho^-$ . To determine  $\phi_2$  requires measuring time-dependent decay rates; here we present such measurements from the Belle [1] and BaBar [2] experiments.

In neutral  $B$  meson decays,  $CP$  violation arises predominantly because of interference between a  $B^0 \rightarrow f$  decay amplitude and a  $B^0 \rightarrow \bar{B}^0 \rightarrow f$  amplitude. For the final states considered here, there are two decay amplitudes possible: a  $b \rightarrow u$  “tree” and a  $b \rightarrow d$  “penguin” (see Fig. 1). Because these amplitudes have different weak phases, additional information is needed to determine  $\phi_2$ , such as the size of the penguin amplitude or the difference in strong phases between the penguin and tree amplitudes.

<sup>1</sup>Charge-conjugate modes are included throughout this paper unless noted otherwise.

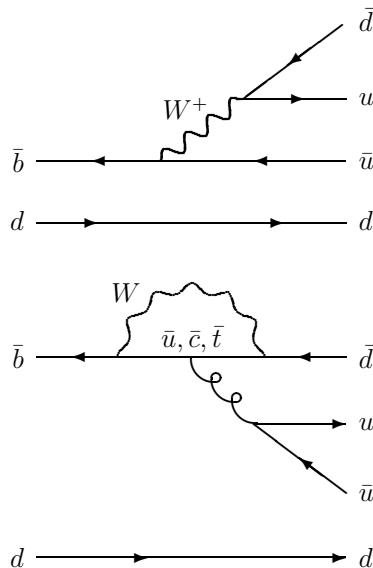


Figure 1. Tree-level diagram (top) and penguin diagram (bottom) for  $B^0 \rightarrow \pi^+\pi^-$ ,  $B^0 \rightarrow \rho^+\pi^-$ , and  $B^0 \rightarrow \rho^+\rho^-$  decays.

## 2. ANALYSIS

The analyses of  $B^0 \rightarrow \pi^+\pi^-$ ,  $B^0 \rightarrow \rho^+\pi^-$ , and  $B^0 \rightarrow \rho^+\rho^-$  decays have several similarities. Events are selected by requiring two opposite-charge pion-candidate tracks originating from the interaction region, and appending zero, one, or two  $\pi^0$ 's. The charged pion identification criteria are based on information from either a DIRC detector (BaBar) [3] or time-of-flight counters and aerogel cherenkov counters (Belle) [4]. Both experiments also use  $dE/dx$  information from the central tracking chamber.

$B$  decays are identified via two kinematic variables: the ‘‘beam-constrained’’ mass,  $m_{bc}$ , and the energy difference,  $\Delta E$ . The former is defined as  $\sqrt{E_b^2 - p_B^2}$  and the latter as  $E_B - E_b$ , where  $p_B$  is the reconstructed  $B$  momentum,  $E_B$  is the reconstructed  $B$  energy, and  $E_b$  is the beam energy, all evaluated in the  $e^+e^-$  center-of-mass (CM) frame. After selection cuts, the  $m_{bc}$  and  $\Delta E$  distributions are jointly fit for the signal event yields. This fit includes contributions from backgrounds, whose  $m_{bc}$ - $\Delta E$  distributions are obtained from either Monte Carlo (MC) simulation or extrapolation from  $m_{bc}$ - $\Delta E$  sidebands.

A tagging algorithm is used to identify the flavor of the  $B$  signal decay, i.e., whether it is  $B^0$  or  $\overline{B}^0$ . This algorithm examines tracks not associated with the signal decay to identify the flavor of the non-signal  $B$ . It depends predominantly on identifying leptons or kaons. The signal-side tracks are fit for a signal decay vertex, and the tag-side tracks are fit for a tag-side decay vertex; the distance  $\Delta z$  between vertices is to good approximation proportional to the time difference between the  $B$  decays:  $\Delta z \approx (\beta\gamma c)\Delta t$ , where  $\beta\gamma$  is the Lorentz boost of the  $e^+e^-$  system and equals 0.43 (0.56) for Belle (BaBar). One subsequently does an unbinned maximum likelihood (ML) fit to  $\Delta t$  to measure or constrain  $\phi_2$ .

The dominant background for all three decays is  $e^+e^- \rightarrow q\bar{q}$  continuum events, where  $q = u, d, s, c$ . To distinguish such events from  $e^+e^- \rightarrow B\overline{B}$  events, the event topology is used: in the CM frame, continuum events tend to be collimated along the beam directions while  $B\overline{B}$  events tend to be spherical. In Belle, the ‘‘shape’’ of an

event is typically quantified via Fox-Wolfram moments [5] of the form  $h_\ell = \sum_{i,j} p_i p_j P_\ell(\cos\theta_{ij})$ , where  $i$  runs over all tracks on the tagging side and  $j$  runs over all tracks on either the tagging side or the signal side. The function  $P_\ell$  is the  $\ell$ th Legendre polynomial and  $\theta_{ij}$  is the angle between momenta  $\vec{p}_i$  and  $\vec{p}_j$ . These moments are combined into a Fisher discriminant [6], and the discriminant is subsequently combined with the probability density function (pdf) for the cosine of the angle between the  $B$  direction and the electron beam direction. This yields an overall likelihood  $\mathcal{L}$ , which is evaluated for both a  $B\overline{B}$  hypothesis and a continuum hypothesis. Signal  $B \rightarrow f$  events are separated from continuum events by cutting on the likelihood ratio  $\mathcal{L}_{B\overline{B}}/(\mathcal{L}_{B\overline{B}} + \mathcal{L}_{q\bar{q}})$ .

In BaBar,  $B \rightarrow f$  signal is separated from continuum background using several methods. For  $B^0 \rightarrow \pi^+\pi^-$ , a cut  $|\cos\theta_{\text{sph}}| < 0.8$  is imposed, where  $\theta_{\text{sph}}$  is the angle between the sphericity axis of the  $B$  candidate and that of the rest of the event. A Fisher discriminant ( $\mathcal{F}$ ) is then constructed from  $\sum_i p_i$  and  $\sum_i p_i |\cos\theta_i|^2$ , where  $p_i$  is the momentum of particle  $i$ ,  $\theta_i$  is the angle between  $\vec{p}_i$  and the  $B$  thrust axis (both evaluated in the  $e^+e^-$  CM frame), and  $i$  runs over all particles not associated with the  $B$  decay. A pdf for  $\mathcal{F}$  is included in the ML fit to  $\Delta t$ . For  $B^0 \rightarrow \rho^+\pi^-$  and one [7] of two  $B^0 \rightarrow \rho^+\rho^-$  analyses, a neural network is used that includes the two event-shape variables from  $\mathcal{F}$ . The output of the neural network is included in the  $\Delta t$  fit. For the other  $B^0 \rightarrow \rho^+\rho^-$  analysis [8], a cut  $|\cos\theta_{\text{th}}| < 0.8$  is made, where  $\theta_{\text{th}}$  is the angle between the thrust axis of the  $B$  candidate and that of the rest of the event. The analysis subsequently uses a Fisher discriminant constructed from 11 observables.

## 3. $B^0 \rightarrow \pi^+\pi^-$

The decay time dependence of  $B^0/\overline{B}^0 \rightarrow \pi^+\pi^-$  decays is given by [9]

$$\frac{dN}{d\Delta t} \propto e^{-\Delta t/\tau} \left[ 1 - q\mathcal{C}_{\pi\pi} \cos(\Delta m\Delta t) + q\mathcal{S}_{\pi\pi} \sin(\Delta m\Delta t) \right], \quad (1)$$

where  $q = +1$  ( $q = -1$ ) corresponds to  $B^0$  ( $\bar{B}^0$ ) tags, and  $\Delta m$  is the  $B^0$ - $\bar{B}^0$  mass difference. The parameters  $\mathcal{C}_{\pi\pi}$  and  $\mathcal{S}_{\pi\pi}$  are  $CP$ -violating and related to  $\phi_2$  via [10]

$$\mathcal{C}_{\pi\pi} = \frac{1}{R} \cdot \left( 2 \left| \frac{P}{T} \right| \sin(\phi_1 - \phi_2) \sin \delta \right) \quad (2)$$

$$\mathcal{S}_{\pi\pi} = \frac{1}{R} \cdot \left( 2 \left| \frac{P}{T} \right| \sin(\phi_1 - \phi_2) \cos \delta + \sin 2\phi_2 - \left| \frac{P}{T} \right|^2 \sin 2\phi_1 \right) \quad (3)$$

$$R = 1 - 2 \left| \frac{P}{T} \right| \cos(\phi_1 + \phi_2) \cos \delta + \left| \frac{P}{T} \right|^2, \quad (4)$$

where  $\phi_1 = (23.2^{+1.6}_{-1.5})^\circ$  [11],  $|P/T|$  is the magnitude of the penguin amplitude relative to that of the tree amplitude, and  $\delta$  is the strong phase difference between the two amplitudes. If there were no penguin contribution,  $P = 0$ ,  $\mathcal{C}_{\pi\pi} = 0$ , and  $\mathcal{S}_{\pi\pi} = \sin 2\phi_2$ . Since Eqs. (2) and (3) have three unknown parameters, measuring  $\mathcal{C}_{\pi\pi}$  and  $\mathcal{S}_{\pi\pi}$  determines a volume in  $\phi_2 - \delta - |P/T|$  space.

The most recent Belle measurement of  $\mathcal{C}_{\pi\pi}$  and  $\mathcal{S}_{\pi\pi}$  is with  $140 \text{ fb}^{-1}$  of data [12]. Candidates must satisfy  $5.271 \text{ GeV}/c^2 < m_{bc} < 5.287 \text{ GeV}/c^2$  and  $\Delta E < 0.064 \text{ GeV}$ ; the final event sample consists of 224  $\bar{B}^0 \rightarrow \pi^+\pi^-$  candidates and 149  $B^0 \rightarrow \pi^+\pi^-$  candidates after background subtraction. The ratio of signal to background is  $\sim 0.3$ . These events are subjected to an unbinned ML fit to  $\Delta t$ , in which additional pdf's and resolution functions are included to account for backgrounds. There are two free parameters in the fit, and the results are  $\mathcal{C}_{\pi\pi} = -0.58 \pm 0.15$  (stat)  $\pm 0.07$  (syst) and  $\mathcal{S}_{\pi\pi} = -1.00 \pm 0.21$  (stat)  $\pm 0.07$  (syst). These values are consistent with previous Belle measurements [13] and indicate large  $CP$  violation. Fig. 2 shows the  $\Delta t$  distributions for the  $q = \pm 1$  samples; a clear difference is seen between the distributions. Many cross-checks have been done for this analysis, including an independent ‘‘blind’’ analysis using a binned ML fit. The latter results are very close to those of the main fit.

The Belle values for  $\mathcal{C}_{\pi\pi}$  and  $\mathcal{S}_{\pi\pi}$  prescribe a 95% C.L. volume in  $\phi_2 - \delta - |P/T|$  space. Slicing this volume at fixed  $|P/T|$  gives a 95% C.L. constraint in the  $\phi_2$ - $\delta$  plane; slicing this volume at

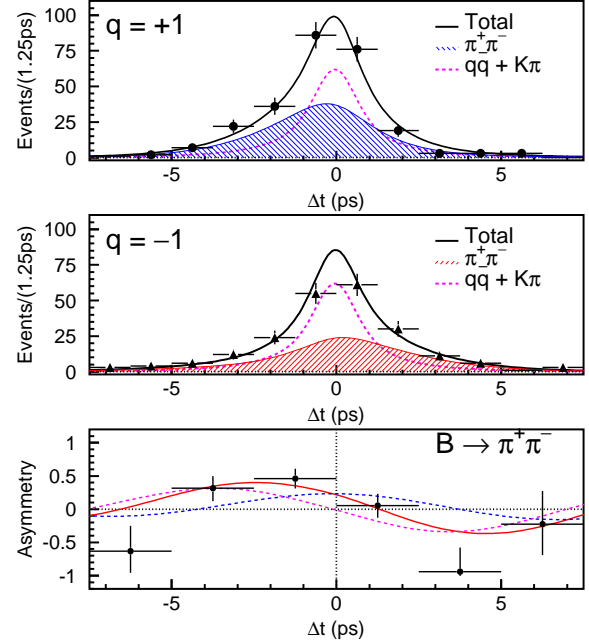


Figure 2. Belle results for  $B^0 \rightarrow \pi^+\pi^-$  [12]: the  $\Delta t$  distributions of  $q = 1$  tags (top),  $q = -1$  tags (middle), and the resulting  $CP$  asymmetry (bottom). The smooth curves are projections of the unbinned ML fit.

fixed  $\delta$  gives a constraint in the  $\phi_2$ - $|P/T|$  plane. Two such projections are shown in Figs. 3a and 3b; the resulting constraints are  $90^\circ < \phi_2 < 146^\circ$  for  $|P/T| < 0.45$  (as predicted by QCD factorization [14] and perturbative QCD [15]), and  $|P/T| > 0.17$  for any value of  $\delta$ .

The BaBar experiment has also measured  $\mathcal{C}_{\pi\pi}$  and  $\mathcal{S}_{\pi\pi}$  using an unbinned ML fit [16]. The most recent result is from  $205 \text{ fb}^{-1}$  of data [17]; the values obtained are  $\mathcal{C}_{\pi\pi} = -0.09 \pm 0.15$  (stat)  $\pm 0.04$  (syst) and  $\mathcal{S}_{\pi\pi} = -0.30 \pm 0.17$  (stat)  $\pm 0.03$  (syst). These values are inconsistent with the Belle result at the level of  $3.2\sigma$  [11]. The BaBar analysis differs from that of Belle in that fewer cuts are made to enrich the data sample; rather, additional pdf's for the discriminating variables are included in the likelihood function. A total of 68 030 events are fit, and a signal yield of  $467 \pm 33$   $B^0 \rightarrow \pi^+\pi^-$  decays is obtained. There are 46 free

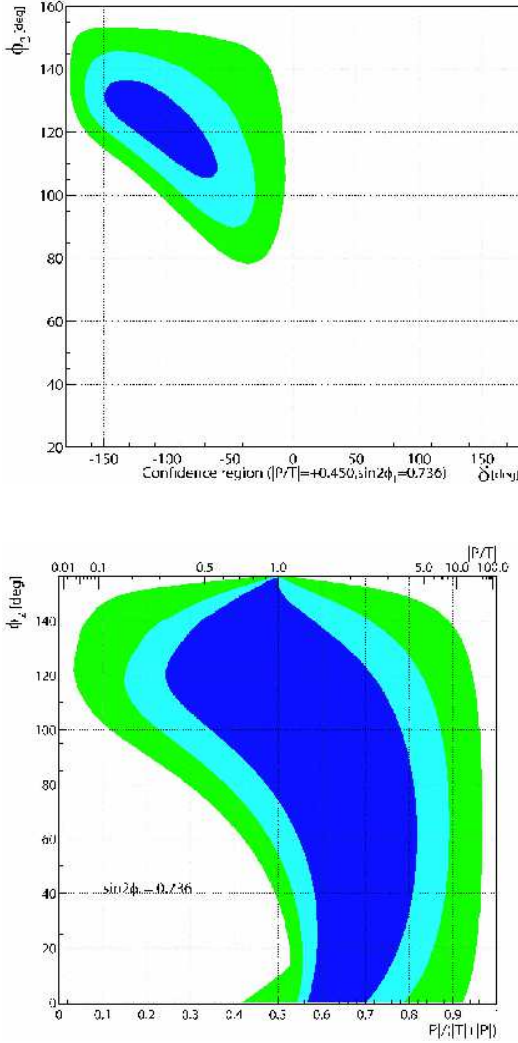


Figure 3. Belle results for  $B^0 \rightarrow \pi^+\pi^-$ : (a) constraints in the  $\phi_2$ - $\delta$  plane for  $|P/T| < 0.45$ ; and (b) constraints in the  $\phi_2$  -  $P/(|P| + |T|)$  plane for all values of  $\delta$ . The dark blue region corresponds to  $1\sigma$  C.L., the light blue region to 90% C.L., and the green region to 95% C.L.

parameters (including  $C_{\pi\pi}$  and  $S_{\pi\pi}$ ) in the fit.

The Belle and BaBar results can be averaged together to constrain  $\phi_2$ . However, such a constraint requires knowledge or assumptions about  $|P/T|$  or  $\delta$ . A model based on  $SU(3)$  symmetry (and including an  $SU(3)$ -breaking factor  $f_K/f_\pi$  for tree amplitudes) and the measured rates for  $B^0 \rightarrow K^0\pi^+$  and  $B^0 \rightarrow K^+\pi^-$  indicates  $\phi_2 = (103 \pm 17)^\circ$  [18] (note: this uses the BaBar result for  $113 \text{ fb}^{-1}$  of data). A preferred method is to use isopin symmetry and the measured rates for  $B^+ \rightarrow \pi^+\pi^0$ ,  $B^0 \rightarrow \pi^0\pi^0$ , and charge-conjugates; this method can determine  $\phi_2$  with little theoretical uncertainty [19]. However, the decay  $B^0 \rightarrow \pi^0\pi^0$  has only recently been observed and the asymmetry between  $B^0$  and  $\bar{B}^0$  measured [20]. Future measurements with higher statistics should yield an interesting constraint on  $\phi_2$ . The overall  $(B^0 + \bar{B}^0) \rightarrow \pi^0\pi^0$  branching fraction can be used to obtain an upper bound [21] on the angular difference  $\theta \equiv \phi_2 - \phi_{2\text{eff}}$ , where  $S_{\pi\pi} = \sin 2\phi_{2\text{eff}}$  (i.e.,  $\phi_{2\text{eff}} \rightarrow \phi_2$  as  $P \rightarrow 0$ ). Using  $C_{\pi\pi}$  and the most recent values of the above branching fractions [11] fluctuated by  $1\sigma$  in the conservative direction, one obtains  $\theta < 36^\circ$ .

#### 4. $B^0 \rightarrow \rho^+\pi^-$

For  $B^0 \rightarrow \rho^+\pi^-$ , the final state is not a  $CP$  eigenstate. There are thus four separate decays to consider:  $B^0 \rightarrow \rho^\pm\pi^\mp$  and  $\bar{B}^0 \rightarrow \rho^\pm\pi^\mp$ . The decay rates can be parametrized as [22]

$$\frac{dN(B \rightarrow \rho^\pm\pi^\mp)}{d\Delta t} \propto (1 \pm A_{CP}^{\rho\pi}) \times e^{-\Delta t/\tau} \left[ 1 - q(C_{\rho\pi} \pm \Delta C_{\rho\pi}) \cos(\Delta m \Delta t) + q(S_{\rho\pi} \pm \Delta S_{\rho\pi}) \sin(\Delta m \Delta t) \right], \quad (5)$$

where  $q = +1$  ( $q = -1$ ) corresponds to  $B^0$  ( $\bar{B}^0$ ) tags. The parameters  $C_{\rho\pi}$  and  $S_{\rho\pi}$  are  $CP$ -violating, while the parameters  $\Delta C_{\rho\pi}$  and  $\Delta S_{\rho\pi}$  are  $CP$ -conserving.  $\Delta C_{\rho\pi}$  characterizes the difference in rates between “ $W \rightarrow \rho$ ” processes  $B^0 \rightarrow \rho^+\pi^-$  or  $\bar{B}^0 \rightarrow \rho^-\pi^+$  and “spectator  $\rightarrow \rho$ ” processes  $B^0 \rightarrow \rho^-\pi^+$  or  $\bar{B}^0 \rightarrow \rho^+\pi^-$  (see Fig. 1).  $\Delta S_{\rho\pi}$  depends, in addition, on differences in

phases between  $W \rightarrow \rho$  and spectator  $\rightarrow \rho$  amplitudes.

The parameter  $A_{CP}^{\rho\pi}$  is equal to the time and flavor integrated asymmetry:  $\Gamma(B^0 \rightarrow \rho^+\pi^-) + \Gamma(\bar{B}^0 \rightarrow \rho^+\pi^-) - \Gamma(\bar{B}^0 \rightarrow \rho^-\pi^+) - \Gamma(B^0 \rightarrow \rho^-\pi^+)$  divided by the sum of the four rates. We also define two separate  $CP$  asymmetries:

$$\begin{aligned} A_{+-} &\equiv \frac{N(\bar{B}^0 \rightarrow \rho^-\pi^+) - N(B^0 \rightarrow \rho^+\pi^-)}{N(\bar{B}^0 \rightarrow \rho^-\pi^+) + N(B^0 \rightarrow \rho^+\pi^-)} \\ &= -\frac{A_{CP}^{\rho\pi} + C_{\rho\pi} + A_{CP}^{\rho\pi} \cdot \Delta C_{\rho\pi}}{1 + \Delta C_{\rho\pi} + A_{CP}^{\rho\pi} \cdot C_{\rho\pi}} \end{aligned} \quad (6)$$

and

$$\begin{aligned} A_{-+} &\equiv \frac{N(\bar{B}^0 \rightarrow \rho^+\pi^-) - N(B^0 \rightarrow \rho^-\pi^+)}{N(\bar{B}^0 \rightarrow \rho^+\pi^-) + N(B^0 \rightarrow \rho^-\pi^+)} \\ &= \frac{A_{CP}^{\rho\pi} - C_{\rho\pi} - A_{CP}^{\rho\pi} \cdot \Delta C_{\rho\pi}}{1 - \Delta C_{\rho\pi} - A_{CP}^{\rho\pi} \cdot C_{\rho\pi}}. \end{aligned} \quad (7)$$

$A_{+-}$  depends only on  $W \rightarrow \rho$  processes and  $A_{-+}$  depends only on spectator  $\rightarrow \rho$  processes.

Both BaBar and Belle have done unbinned ML fits to the  $\Delta t$  distributions of  $B^0 \rightarrow \rho^\pm \pi^\pm$  decays to determine  $A_{CP}^{\rho\pi}$ ,  $C_{\rho\pi}$ ,  $S_{\rho\pi}$ ,  $\Delta C_{\rho\pi}$ ,  $\Delta S_{\rho\pi}$ ,  $A_{+-}$ , and  $A_{-+}$ . The Belle analysis is with  $140 \text{ fb}^{-1}$  of data [23]; the BaBar analysis, originally with  $81 \text{ fb}^{-1}$  of data [24], has been updated with  $113 \text{ fb}^{-1}$  [25].

To remove charge-ambiguous decays and possible interference between  $B^0 \rightarrow \rho^+\pi^-$  and  $B^0 \rightarrow \rho^-\pi^+$  amplitudes, one must eliminate the overlap region of the  $\pi^+\pi^-\pi^0$  Dalitz plot. Belle does this by requiring  $0.57 \text{ GeV}/c^2 < m_{\pi^\pm\pi^0} < 0.97 \text{ GeV}/c^2$  and  $m_{\pi^\mp\pi^0} > 1.22 \text{ GeV}/c^2$ . BaBar makes the looser selection  $0.40 \text{ GeV}/c^2 < m_{\pi^\pm\pi^0} < 1.30 \text{ GeV}/c^2$  and requires that  $m_{\pi^\mp\pi^0}$  not be in this range. In addition, BaBar requires that the bachelor track from  $B \rightarrow \rho\pi$  has  $p > 2.4 \text{ GeV}/c$ , where  $p$  is evaluated in the  $e^+e^-$  CM frame; only 14% of pions from (selected)  $\rho^\pm$  decays satisfy this requirement. Finally, Belle requires  $m_{\pi^+\pi^-} > 0.97 \text{ GeV}/c^2$  to avoid the overlap region between  $B^0 \rightarrow \rho^0\pi^0$  and  $B^0 \rightarrow \rho^\pm\pi^\mp$ .

Belle subsequently defines a signal region  $m_{bc} > 5.27 \text{ GeV}/c^2$  and  $-0.10 \text{ GeV} < \Delta E < 0.08 \text{ GeV}$ . There are 1215 events in this region that pass all selection requirements. Fitting to the  $m_{bc}-\Delta E$  distributions yields 329  $B^0 \rightarrow \rho^+\pi^-$

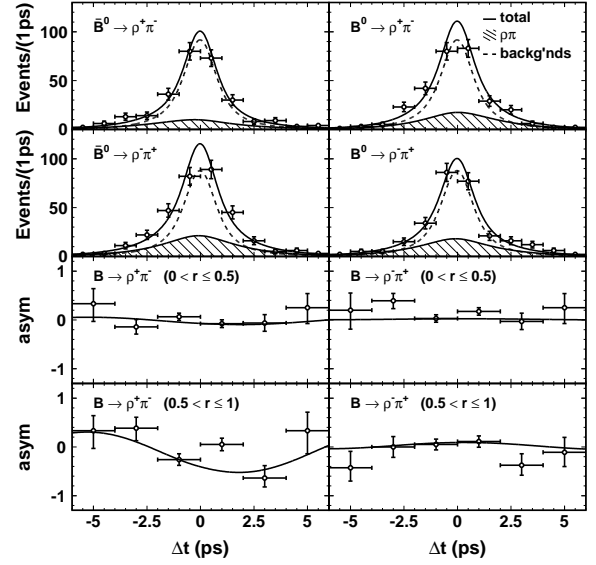


Figure 4. Belle results for  $B^0 \rightarrow \rho^+\pi^-$  [23]: the  $\Delta t$  distributions of  $q = 1$  tags (left),  $q = -1$  tags (right), and the resulting  $CP$  asymmetry (bottom rows). The asymmetry is shown separately for high-quality tags ( $r > 0.5$ ) and low quality tags ( $r < 0.5$ ). The smooth curves are projections of the unbinned ML fit.

candidates. The resulting  $\Delta t$  distributions for  $q = \pm 1$  tagged events are shown in Fig. 4 along with projections of the unbinned ML fit in  $\Delta t$ . Also shown is the  $CP$  asymmetry, which is consistent with zero.

The BaBar results are similar to those from Belle; the corresponding  $\Delta t$  distributions and  $CP$  asymmetry are shown in Fig. 5. All Belle and BaBar results are listed in Table 1. There is very good agreement between the measurements except for  $\Delta S_{\rho\pi}$ , where the disagreement is  $\sim 2\sigma$ . A recent BaBar analysis with  $192 \text{ fb}^{-1}$  of data [26] uses a different strategy than the quasi-two-body approach: it takes advantage of interference in the  $\pi^+\pi^-\pi^0$  Dalitz plot as prescribed in Ref. [27]. These results are also listed in Table 1 for comparison; they are very similar to those from the quasi-two-body analyses.

These measured values can be used to constrain

Table 1  
Results of fits to the  $\Delta t$  distributions for  $B^0 \rightarrow \rho^+ \pi^-$  candidates.

	Belle 2-body (140 fb <sup>-1</sup> )	BaBar 2-body (113 fb <sup>-1</sup> )	BaBar Dalitz (192 fb <sup>-1</sup> )
$A_{CP}^{\rho\pi}$	$-0.16 \pm 0.10 \pm 0.02$	$-0.114 \pm 0.062 \pm 0.027$	$-0.088 \pm 0.049 \pm 0.013$
$C_{\rho\pi}$	$0.25 \pm 0.17^{+0.02}_{-0.06}$	$0.35 \pm 0.13 \pm 0.05$	$0.34 \pm 0.11 \pm 0.05$
$S_{\rho\pi}$	$-0.28 \pm 0.23^{+0.10}_{-0.08}$	$-0.13 \pm 0.18 \pm 0.04$	$-0.10 \pm 0.14 \pm 0.04$
$\Delta C_{\rho\pi}$	$0.38 \pm 0.18^{+0.02}_{-0.04}$	$0.20 \pm 0.13 \pm 0.05$	$0.15 \pm 0.11 \pm 0.03$
$\Delta S_{\rho\pi}$	$-0.30 \pm 0.24 \pm 0.09$	$0.33 \pm 0.18 \pm 0.03$	$0.22 \pm 0.15 \pm 0.03$
$A_{+-}$	$-0.02 \pm 0.16^{+0.05}_{-0.02}$	$-0.18 \pm 0.13 \pm 0.05$	$-0.21 \pm 0.11 \pm 0.04$
$A_{-+}$	$-0.53 \pm 0.29^{+0.09}_{-0.04}$	$-0.52^{+0.17}_{-0.19} \pm 0.07$	$-0.47^{+0.14}_{-0.15} \pm 0.06$

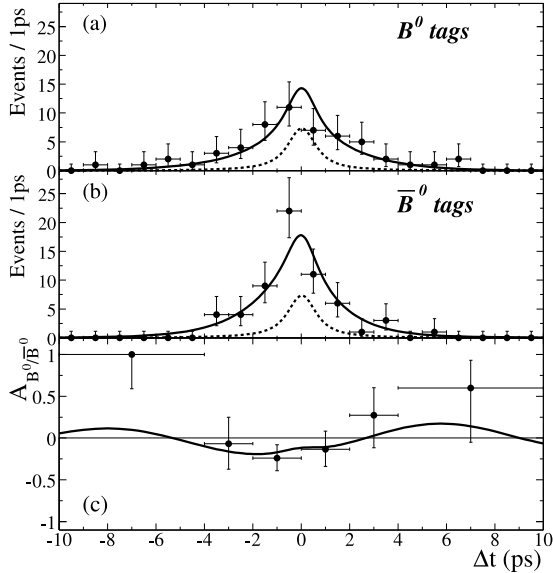


Figure 5. BaBar results for  $B^0 \rightarrow \rho^+ \pi^-$  [24]: the  $\Delta t$  distributions of  $q = 1$  tags (top),  $q = -1$  tags (middle), and the resulting  $CP$  asymmetry (bottom). The smooth curves are projections of the unbinned ML fit.

$\phi_2$ ; however, since the penguin contribution is unknown, additional information is needed. A recent theoretical model [28] uses  $SU(3)$  symmetry and the measured rates or limits for branching fractions of  $B^0 \rightarrow K^{*\pm} \pi^\mp$ ,  $B^0 \rightarrow \rho^\mp K^\pm$ ,  $B^\pm \rightarrow K^{*0} \pi^\pm$ , and  $B^\pm \rightarrow \rho^\pm K^0$ .  $SU(3)$ -breaking effects are considered at tree level and accounted for via a factor  $f_\pi/f_K$ . The strong phase difference between the two tree amplitudes ( $W \rightarrow \rho$  and spectator  $\rightarrow \rho$ ) is assumed to be small, as predicted by factorization. The resulting central values and errors for  $\phi_2$  are:  $102 \pm 19^\circ$  for Belle values of  $C_{\rho\pi}$ ,  $S_{\rho\pi}$ ,  $\Delta C_{\rho\pi}$ ,  $\Delta S_{\rho\pi}$ ;  $93 \pm 17^\circ$  for BaBar values (113 fb<sup>-1</sup>); and  $95 \pm 16^\circ$  for Belle and BaBar values combined.

The BaBar Dalitz plot analysis (192 fb<sup>-1</sup>) [26] allows one to directly fit for  $\phi_2$  with little theoretical uncertainty from the penguin contribution. The result is  $\phi_2 = (113^{+27}_{-17}(\text{stat}) \pm 6(\text{syst}))^\circ$ , consistent with the  $SU(3)$ -based results above.

## 5. $B^0 \rightarrow \rho^+ \rho^-$

The decay  $B^0 \rightarrow \rho^+ \rho^-$  has two vector particles in the final state. If the  $\rho$  mesons are longitudinally polarized,  $\ell$  is even and  $CP = +1$ ; but if they are transversely polarized,  $\ell$  can be even or odd and the final state is not a  $CP$  eigenstate.

For longitudinal polarization,  $\phi_2$  can be determined from the  $\Delta t$  distribution as done for  $B^0 \rightarrow \pi^+ \pi^-$ . However,  $B^0 \rightarrow \rho^+ \rho^-$  has an advantage: the penguin contribution is expected to be small relative to the tree contribution [29], which

reduces theoretical uncertainty on  $\phi_2$ . Unfortunately  $B^0 \rightarrow \rho^+ \rho^-$  is more challenging experimentally: there are several backgrounds and also possible nonresonant contributions. The method depends upon the  $\rho$ 's being longitudinally polarized; otherwise a more involved angular analysis is necessary to determine  $\phi_2$  [30]. Finally, the nonnegligible decay width of the  $\rho$  allows for  $I = 1$  final states, which complicates extracting  $\phi_2$  via an isospin analysis [31].

The decay  $B^0 \rightarrow \rho^+ \rho^-$  has been observed by BaBar and the  $CP$ -violating parameters  $\mathcal{C}_{\rho\rho}$  and  $\mathcal{S}_{\rho\rho}$  measured with  $81 \text{ fb}^{-1}$  of data [7,8] and updated with  $113 \text{ fb}^{-1}$  of data [25]. A similar analysis is underway at Belle with  $250 \text{ fb}^{-1}$  of data. The final state consists of four pions, two charged and two neutral. In the case of multiple  $B^0 \rightarrow \rho^+ \rho^-$  candidates arising from multiple  $\pi^0$  candidates, the candidate that minimizes the sum  $\sum_i (m_{\gamma\gamma}^{(i)} - m_{\pi^0})$  is chosen, where  $i$  runs over the  $\rho^\pm$  candidates. From MC simulation, it is found that one or more pions from  $B^0 \rightarrow \rho^+ \rho^-$  are swapped with pions from the tag side 39% (16%) of the time for longitudinal (transverse) polarization.

BaBar selects events with relatively loose cuts and does an unbinned ML fit to the  $\Delta t$  distribution, including pdf's to account for backgrounds. Nonresonant contributions and interference with decays yielding the same final state, e.g.,  $B^0 \rightarrow a_1 \pi^0$ , are estimated to be small and neglected. For  $81 \text{ fb}^{-1}$  of data, 24 288 events are fit and a signal yield of  $224 \pm 29$  is obtained. The fit includes a pdf for the angles  $\theta_1$  and  $\theta_2$ , where  $\theta_i$  is the angle between the  $\pi^0$  from  $\rho_i^\pm \rightarrow \pi^\pm \pi^0$  and the  $B^0$  in the  $\rho_i^\pm$  rest frame ( $i = 1, 2$ ). This pdf has the form [32]

$$\frac{d^2\Gamma}{\Gamma d\cos\theta_1 d\cos\theta_2} = \frac{9}{4} \left\{ f_L \cos^2\theta_1 \cos^2\theta_2 + \left( \frac{1-f_L}{4} \right) \sin^2\theta_1 \sin^2\theta_2 \right\} \quad (8)$$

and determines  $f_L$ , the fraction of longitudinally polarized decays. The fit results are  $\mathcal{C}_{\rho\rho} = -0.23 \pm 0.24 \pm 0.14$  and  $\mathcal{S}_{\rho\rho} = -0.19 \pm 0.33 \pm 0.11$  ( $113 \text{ fb}^{-1}$ ), and  $f_L = 0.99 \pm 0.03_{-0.03}^{+0.04}$  ( $81 \text{ fb}^{-1}$ ). The first error listed is statistical and the second

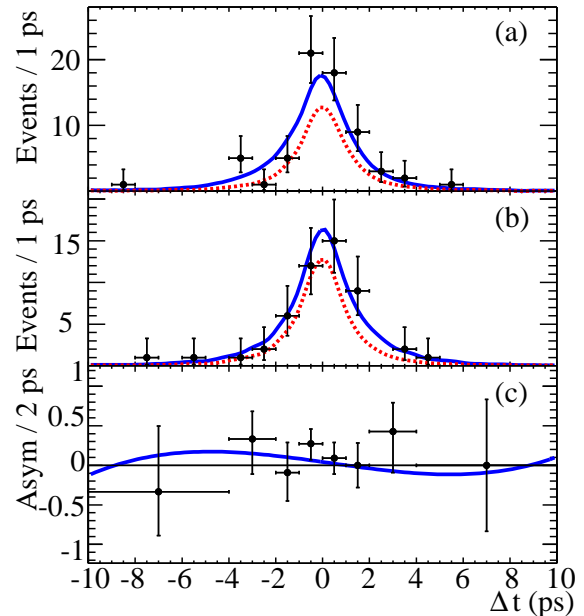


Figure 6. BaBar results for  $B^0 \rightarrow \rho^+ \rho^-$  [7]: the  $\Delta t$  distributions of  $q = 1$  tags (top),  $q = -1$  tags (middle), and the resulting  $CP$  asymmetry (bottom). The smooth curves are projections of the unbinned ML fit.

systematic.

It is fortunate that  $f_L$  is close to unity; in this case the final state has  $CP = +1$  and an angular analysis to determine  $\phi_2$  is unnecessary. Fig. 6 shows the  $\Delta t$  distributions for  $q = \pm 1$  tagged events along with the resulting  $CP$  asymmetry. No  $CP$  violation is observed. Inputting the measured values for  $\mathcal{C}_{\rho\rho}$  and  $\mathcal{S}_{\rho\rho}$  into an isospin analysis that includes the branching fractions for  $B^0 \rightarrow \rho^+ \rho^-$  [7] and  $B^+ \rightarrow \rho^+ \rho^0$  [33], and the upper limit for  $B(B^0 \rightarrow \rho^0 \rho^0)$  [34], one obtains  $\phi_2 = (96 \pm 10 \text{ (stat)} \pm 4 \text{ (syst)} \pm 11_{\text{theory}})^\circ$  [35]. The last error is due to the penguin contribution; it is significantly smaller than that for  $B \rightarrow \pi\pi$  ( $\pm 36^\circ$ ), as expected.

## 6. SUMMARY

Time-dependent  $CP$  asymmetries in  $B^0 \rightarrow \pi^+ \pi^-$ ,  $B^0 \rightarrow \rho^+ \pi^-$ , and  $B^0 \rightarrow \rho^+ \rho^-$  decays are

measured and used to constrain the CKM angle  $\phi_2$ . The  $B^0 \rightarrow \pi^+\pi^-$  mode is experimentally clean but has the largest penguin contribution, which contributes theoretical uncertainty to  $\phi_2$ . A model-independent constraint is  $90^\circ < \phi_2 < 146^\circ$  for  $|P/T| < 0.45$  (95% C.L.). An  $SU(3)$ -based model [18] indicates  $\phi_2 = (103 \pm 17)^\circ$  (and also that  $|P/T|$  is large). Belle observes large  $CP$  violation in this mode while BaBar does not.

The  $B^0 \rightarrow \rho^\pm\pi^\mp$  mode is more complicated as there are more backgrounds than for  $B^0 \rightarrow \pi^+\pi^-$  and the final state is not a  $CP$  eigenstate. A model based upon  $SU(3)$  symmetry and using the measured branching fractions for  $B \rightarrow K^*\pi^\pm$  and  $B \rightarrow \rho^\pm K$  obtains  $\phi_2 = 95 \pm 16^\circ$  (Belle + BaBar quasi-two-body results combined).

The  $B^0 \rightarrow \rho^+\rho^-$  mode has the smallest penguin contribution but suffers from additional backgrounds, possible nonresonant contributions, and a possible  $I = 1$  component in the final state. Neglecting the latter two effects, BaBar measures  $\mathcal{C}_{\rho\rho}$  and  $\mathcal{S}_{\rho\rho}$  for longitudinal polarization, which dominates the decay. Combining the measured values with the branching fractions or limits for  $B^0 \rightarrow \rho^+\rho^-$  [7],  $B^+ \rightarrow \rho^+\rho^0$  [33], and  $B^0 \rightarrow \rho^0\rho^0$  [34] gives  $\phi_2 = (96 \pm 10(\text{stat}) \pm 4(\text{syst}) \pm 11_{\text{theory}})^\circ$  [35]. This value is similar to those obtained from measurements of  $B^0 \rightarrow \pi^+\pi^-$  and  $B^0 \rightarrow \rho^\pm\pi^\mp$  decays.

## REFERENCES

1. <http://belle.kek.jp/>
2. <http://www.slac.stanford.edu/BFR00T/>
3. B. Aubert *et al.*, Nucl. Instr. Meth. A 479 (2002) 1.
4. A. Abashian *et al.*, Nucl. Instr. Meth. A 479 (2002) 117.
5. G. C. Fox and S. Wolfram, Phys. Rev. Lett. 41 (1978) 1581.
6. B. Casey *et al.*, Phys. Rev. D 66 (2002) 092002.
7. B. Aubert *et al.*, Phys. Rev. D 69 (2004) 031102.
8. B. Aubert *et al.*, hep-ex/0404029 (2004).
9. M. Gronau, Phys. Rev. Lett. 63 (1989) 1451.
10. M. Gronau and J. L. Rosner, Phys. Rev. D 65 (2002) 093012.
11. <http://www.slac.stanford.edu/xorg/hfag/>
12. K. Abe *et al.*, Phys. Rev. Lett. 93 (2004) 021601.
13. K. Abe *et al.*, Phys. Rev. D 68 (2003) 012001.
14. M. Beneke *et al.*, Nucl. Phys. B 606 (2001) 245; M. Beneke and M. Neubert, Nucl. Phys. B 675 (2003) 333.
15. Y. Y. Keum and A. A. Sanda, Phys. Rev. D 67 (2003) 054009.
16. B. Aubert *et al.*, Phys. Rev. Lett. 89 (2002) 281802.
17. B. Aubert *et al.*, hep-ex/0408089 (2004).
18. M. Gronau and J. L. Rosner, Phys. Lett. B 595 (2004) 339.
19. M. Gronau and D. London, Phys. Rev. Lett. 65 (1990) 3381.
20. K. Abe *et al.*, hep-ex/0408101 (2004).
21. M. Gronau *et al.*, Phys. Lett. B 514 (2001) 315; J. Charles, Phys. Rev. D 59 (1999) 054007; Y. Grossman and H. R. Quinn, Phys. Rev. D 58 (1998) 017504.
22. M. Gronau, Phys. Lett. B 233 (1989) 479.
23. C. C. Wang *et al.*, hep-ex/0408003 (2004).
24. B. Aubert *et al.*, Phys. Rev. Lett. 91 (2003) 201802.
25. L. Roos (for BaBar), hep-ex/0407051 (2004).
26. B. Aubert *et al.*, hep-ex/0408099 (2004).
27. H. R. Quinn and A. E. Snyder, Phys. Rev. D 48 (1993) 2139.
28. M. Gronau and J. Zupan, hep-ph/0407002 (2004).
29. R. Aleksan *et al.*, Phys. Lett. B 356 (1995) 95.
30. I. Dunietz *et al.*, Phys. Rev. D 43 (1991) 2193.
31. A. F. Falk *et al.*, Phys. Rev. D 69 (2004) 011502.
32. K. Abe, M. Satpathy, and H. Yamamoto, hep-ex/0103002 (2001).
33. J. Zhang *et al.*, Phys. Rev. Lett. 91 (2003) 221801; B. Aubert *et al.*, Phys. Rev. Lett. 91 (2003) 171802.
34. B. Aubert *et al.*, hep-ex/0408061 (2004).
35. M. A. Giorgi, "Recent Results on CP Violation in B Decays," presented at XXXII Int. Conf. on High Energy Physics, Beijing, China, 16-22 August 2004.